Hindawi
Journal of Nanotechnology
Volume 2018, Article ID 9504807, 10 pages
https://doi.org/10.1155/2018/9504807

Research Article

Biosynthesis of Multicomponent Nanoparticles with Extract of Mortiño (*Vaccinium floribundum* Kunth) Berry: Application on Heavy Metals Removal from Water and Immobilization in Soils

Mayra Abril,[1] Hugo Ruiz,[2] and Luis H. Cumbal[1,2]

[1]*Departamento de Ciencias de la Vida, Universidad de las Fuerzas Armadas ESPE, Av. Gral. Rumiñahui s/n, P.O. Box 171-5-231B, Sangolquí, Ecuador*
[2]*Centro de Nanociencia y Nanotecnología, Universidad de las Fuerzas Armadas ESPE, Av. Gral. Rumiñahui s/n, P.O. Box 171-5-231B, Sangolquí, Ecuador*

Correspondence should be addressed to Luis H. Cumbal; lhcumbal@espe.edu.ec

Received 19 October 2017; Accepted 31 January 2018; Published 1 April 2018

Academic Editor: Andrey E. Miroshnichenko

Through preparation of multicomponent nanoparticles (MCNPs) using ferric chloride ($FeCl_3$), sodium sulfate (Na_2SO_4), and the extract of mortiño fruit (*Vaccinium floribundum* Kunth), we dramatically improved the removal/immobilization of heavy metals from water and in soils. As-prepared nanoparticles were spherical measuring approximately 12 nm in diameter and contained iron oxides and iron sulfides in the crystal structure. Removal of copper and zinc from water using MCNPs showed high efficiencies (>99%) at pH above 6 and a ratio of 0.5 mL of the extract:10 mL 0.5 M $FeCl_3{\cdot}6H_2O$: 10 mL 0.035 M Na_2SO_4. The physisorption process followed by chemisorption was regarded as the removal mechanism of Cu and Zn from water. While, when MCNPs were used to treat soils contaminated with heavy metals, more than 95% of immobilization was accomplished for all metals. Nevertheless, the distribution of the metallic elements changed in the soil fractions after treatment. Results indicate that immobilization of metals after the injection of nanoparticles into soils was effective. Metals did not leach out when soils were drained with rain, drinking, and deionized water but fairly leached out under acidic water drainage.

1. Introduction

In this century, the applications of nanotechnology are increasing, particularly those related to the use of nanoparticles (NPs). All NPs show outstanding physical, mechanical, optical, catalytic, and chemical properties due to a variety of morphologies, sizes, and reactivities [1–3]. Even though the current NPs have found broader and potential applications in the fields of medicine, energy, cosmetics, environmental remediation, and catalysis, an enormous amount of hazardous chemicals have been used in their synthesis [4]. A massive quantity of fabricated nanoparticles includes only a single element, but more beneficial properties can be attained when the nanoparticles contain two or more dissimilar elements that altogether form multicomponent nanoparticles (MCNPs). The inclusion of two or more components can add supplementary functionality to the particles, such as antimicrobial activity, chemical-mechanical polishing [5], magnetic capability [6], and others. Among the MCNPs prepared up to now, Fe/FeS nanoparticles were formed by the interaction between dissolved iron species and hydrogen sulfide using sodium borohydride ($NaBH_4$) as a reducing agent at room temperature [7]. Using this procedure of fabrication, the FeS precipitates on the Fe^0 surface. These nanoparticles were successfully used in the removal of trichloroethylene and pesticides from water. Similar nanoparticles were prepared using sodium sulfate instead of dithionite to selectively immobilize heavy metals from the aqueous phase [8]. In both studies, the performance of the MCNPs was excellent; however, researchers used $NaBH_4$ as the reducing agent. This chemical is expensive, hazardous, and harmful to the ecosystem [9, 10]. On the contrary, in this research, we exploit green nanoscience to

reduce the risks of using nanomaterials on human health and the environment.

With the evolution of green chemistry, ecofriendly dispersing agents such as polymers and oligomers have increasingly been used for the stabilization of multicomponent nanoparticles [5]. Natural products like plant extracts have attracted attention for this purpose because they are easy to handle, readily available, low cost, and highly biocompatible, and their own polyphenols (e.g., flavonoids and flavones), carotenoids, reducing sugars, glucosinolates, terpenoids, glutathiones, metallothioneins, and so on are ecological [11–14].

Mortiño (*Vaccinium floribundum*), sometimes called Andean berry, belongs to the Ericaceae family. The fruit is round, is bluish black in color, and is about 8 mm in diameter. The berry grows in a shrub 1.5 m tall, with lanceolate leaves 2 cm long possessing a serrated edge. In Ecuador, it grows in high altitudes, between 3400 and 3800 meters above the sea level. It is a well-known fruit because of its high antioxidant activity for the presence of anthocyanins (delphinine, peonidin, malvidin, and cyanidin) and other phenolic compounds (quercetin, myricetin, gallic acid, ellagic acids, hydroxycinnamic and hydroxybenzoic acid derivatives, and others) in very high concentrations. The berry is consumed fresh, dried, in sausages, jellies, and jams, and in a special beverage called "colada morada" [15, 16]. Furthermore, mortiño contains a high content of glucose and fructose. In this research, we use the mortiño berry extract (MBE) as a reducing and stabilizing agent in the synthesis of MCNPs.

2. Experimental Section

2.1. Materials. Chemicals purchased from Fisher Scientific were ferric chloride ($FeCl_3{\cdot}6H_2O$, 99.8%), sodium sulfate (Na_2SO_4, 99.9%), ascorbic acid (USP/FCC), hydrochloric acid (HCl, 37.3%), nitric acid (HNO_3, 69.5%), sodium hydroxide (NaOH, 98%), and buffer solution (0.2 M sodium acetate, 96%) and from HiMedia were potassium iodide (KIO_3, 99%). Fresh and ripe mortiño berries were purchased in a nearby popular market. Millipore Milli-Q water was used in all experiments.

2.2. Preparation of the Mortiño Extract. First, fresh mortiño berries were washed with Milli-Q and cut into small pieces. Then, 300 grams of crushed mortiño fruit were immersed in 300 mL of 99.6% ethanol for 2 days. The resultant solution was filtered using the Whatman no.1 paper and dried at 40°C under reduced pressure and then freeze-dried for 24 hours to give a dark reddish gummy extract.

2.3. Biosynthesis of Multicomponent Nanoparticles. 10 mL of 0.5 M $FeCl_3{\cdot}6H_2O$ was used as an iron source. The pH of the solution was adjusted to 8.7 with 0.1 M NaOH, and the resulting suspension was centrifuged at 3000 rpm for 10 min. The supernatant was discarded, and 10 mL of 0.035 M Na_2SO_4 was added to the Fe precipitate. Afterwards, the mixture was stirred, and the concentrated fruit extract was added, keeping a ratio of 10 : 10 : 0.5 (v/v/v) for ferric chloride, sodium sulfate, and MBE.

2.4. Characterization. The particle size distribution of MCNPs was determined using the HORIBA, DLS Version LB-550 program. Transmission electron microscope images were digitally recorded (Tecnai G2 Spirit TWIN, FEI, Holland). XRD studies on thin films of the nanoparticle were carried out using a diffractometer (EMPYREAN, PANalytical) with a θ–2θ configuration (generator-detector), wherein a copper X-ray tube emitted a wavelength of $\lambda = 1.54$ Å. FTIR-ATR spectra were recorded on a Spectrum Two IR spectrometer (PerkinElmer, USA) to detect the different functional groups involved in the capture of heavy metals by the multicomponent nanoparticles. The UV-Vis spectrum was obtained using a spectrophotometer (Analytik Jena SPECORD S6008, Germany).

2.5. Removal of Heavy Metals. Batch kinetic tests for heavy metal removal from the liquid phase after treatment with nanoparticles were carried out using 100 mL Boeco bottles under the oxidant environment and pH 6.5 ± 0.2. The removal was initiated by mixing 1 mL of MCNPs with 10 mL of artificially contaminated water, which resulted in concentrations of 5.2 mg/L Cu^{2+}, 4.95 mg/L Zn^{2+}, 4.05 mg/L Mn^{2+}, 2.51 mg/L Ni^{2+}, 2.98 mg/L Cd^{2+}, and 1.12 mg/L Cr^{6+}. Bottles were placed in a water bath and agitated for 2.5 h at 25°C. During the test, six samples of 2 mL of the treated aqueous phase were filtered with a 0.2 μm PVDF filter for heavy metal analyses at 5, 20, 40, 60, 120, and 150 min.

2.6. Soil Characterization. Cation exchange capacity of the soil was performed using the 9081 EPA method. Briefly, the soil sample was saturated with a solution of 1.0 N of sodium acetate to replace cations bound to the soil with sodium ions at pH 8.2. The sample was then placed on a rotary shaker at 40 rpm for 1.0 h and centrifuged for 5 min, and the supernatant decanted. The precipitate was washed 5 times with 99% isopropyl alcohol. Then, 100 mL of 1.0 N ammonium acetate at pH 7 was added, and the content was placed on the rotary shaker at 40 rpm for another hour and centrifuged. A sample of 1 mL was taken from the supernatant diluted with 9.0 mL of ammonium acetate and filtered with a membrane of 0.45 μm, and the sodium concentration was analyzed by atomic absorption. The organic matter contained in the soil was measured using the method reported by [17]. After oven-drying of soil to constant weight (12–24 h at 105°C), 10 g of dry soil was weighed in a porcelain dish (DW_{105}) and placed in a Wild Barfield muffle, model MI 254, at 550°C for six hours. After total calcination, the sample was allowed to cool down and weighed again, and the value was recorded (DW_{550}). The organic matter content was estimated with the following equation:

$$\mathrm{OM} = \frac{\mathrm{DW}_{105} - \mathrm{DW}_{550}}{\mathrm{DW}_{105}} * 100. \quad (1)$$

For the doping of soil with heavy metals, deionized water containing different concentrations of Cu^{2+}, Zn^{2+}, Ni^{2+}, Mn^{2+},

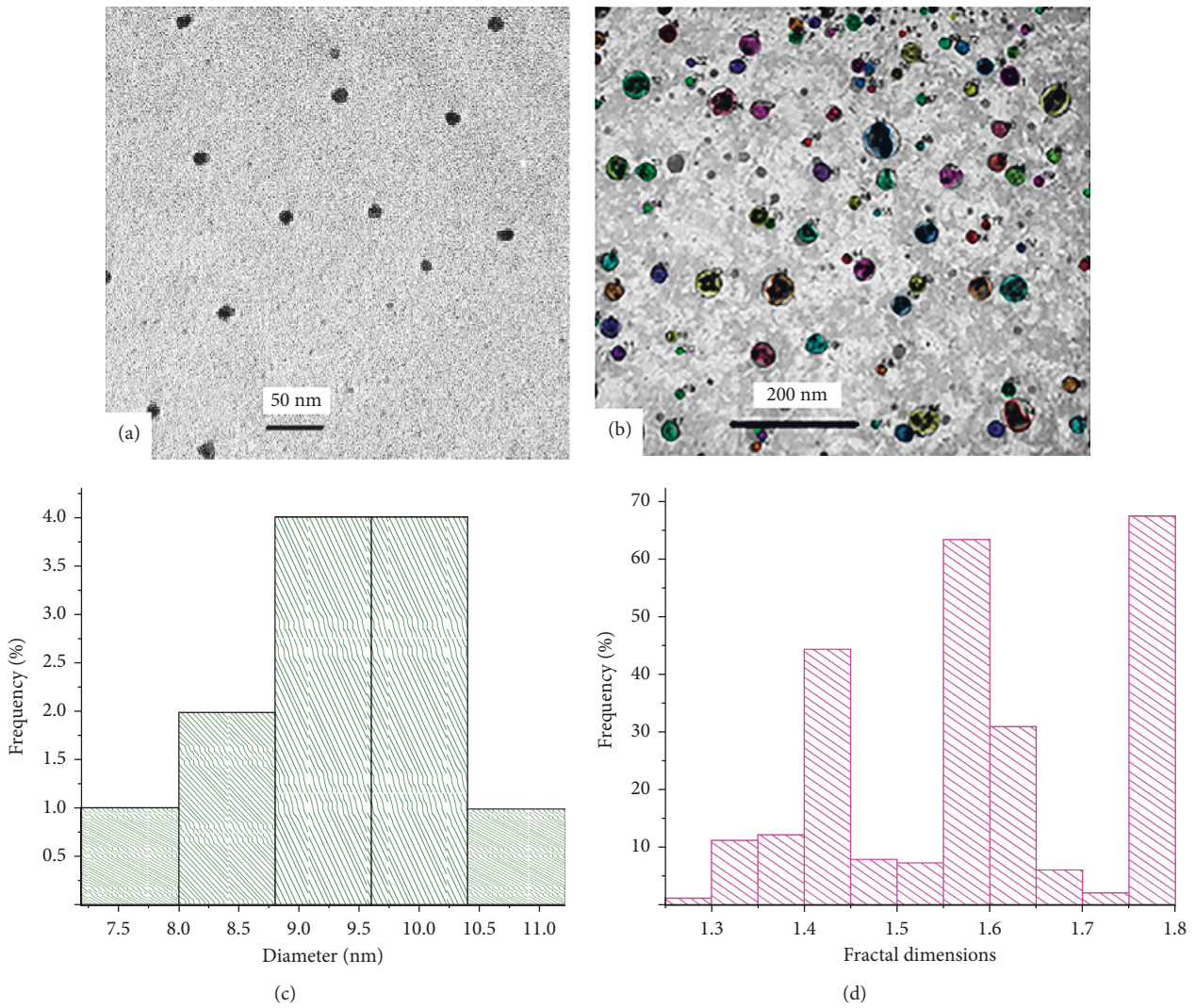

Figure 1: Multicomponent nanoparticles synthesized with the mortiño berry extract: (a) TEM image, (b) TEM image analyzed with MATLAB software, (c) DLS size distribution, and (d) fractal roughness.

Cd^{2+}, and Cr^{6+} was used to saturate 521.8 g of soil taken from a mining site with a continuous agitation for four days. Afterwards, the soil sample was centrifuged at 3000 rpm for 10 min, and the supernatant was separated. The remaining solids were washed twice with distilled water to remove the soluble fraction of heavy metals. Finally, the supernatant and washed fractions were filtered through a membrane filter of 0.45 μm, and the dissolved metal concentrations were measured using an atomic absorption spectrometer by the flame method. Doped soil reached concentrations of 636 mg/kg Cu^{2+}, 737 mg/kg Zn^{2+}, 21.2 mg/kg Ni^{2+}, 408 mg/kg Mn^{2+}, 19.2 mg/kg Cd^{2+}, and 195 mg/kg Cr^{6+}.

2.7. Immobililization Tests. Experiments of immobilization of heavy metals were performed by adding dropwise different volumes of MCNPs at pH 6.5 ± 0.2 (5, 10, 15, and 20 mL) into a glass chromatographic column packed with 2.0 g of previously doped soils. Concentrations of heavy metals in soil samples, before and after treatment, were obtained using a sequential extraction method [18]. The extraction was performed consecutively on an initial weight of 1.0 g of soil, following a three-step procedure: Step 1: for the exchangeable-weakly sorbed, 20 mL of 0.11 M acetic acid was added to 1.0 g of soil sample in a Falcon tube and shaken for 16 h at room temperature. The extract was then separated from the solid residue by centrifugation at 3000 rpm for 20 min, and the supernatant liquid was filtrated with a 0.45 μm membrane. Subsequently, the filtrate was chemically analyzed by atomic absorption to measure concentration of heavy metals. The solid residue was washed by adding 20 mL of deionized water, shaken for 15 min, and centrifuged at 3000 rpm for 20 min. Step 2: heavy metals bound to Fe/Mn oxides were extracted by adding 40 mL of 0.1 M hydroxylamine hydrochloride to the residue from Step 1 and resuspended by mechanical shaking for 16 h at room temperature. The separation of the extract, filtration of the supernatant, analysis of the filtrate, and rinsing of residues were carried out

as indicated in Step 1. In Step 3: heavy metals strongly bound or incorporated into organic matter or other oxidizable species. The residue from Step 2 was treated twice with 10 mL of 8.8 M hydrogen peroxide (H_2O_2). Then, the digestion was allowed to proceed at room temperature for 1.0 h with occasional manual agitation, followed by digestion for another hour at $85 \pm 1^{\circ}$C in a water bath. During the digestion, the Falcon tube was loosely capped to avoid loss of hydrogen peroxide. Next, the tube was uncapped, and heating was continued until the volume decreased to approximately 2-3 mL. An additional 10 mL of peroxide was added to the tube, capped, and digested at $85 \pm 1^{\circ}$C for 1.0 h. Heating continued as before until the volume was reduced to 2-3 mL. Finally, 25 mL of 1.0 M ammonium acetate was added to the cold mixture and shaken for 16 h at room temperature. The separation of the extract, filtration of the supernatant, analysis of the filtrate, and rinsing of residues were carried out as described in Step 1. Heavy metals sorbed or carbonate-bound were discarded in this study because the amount of carbonates in soil were insignificant.

2.8. Chemical and Physical Analyses. Almost all heavy metals (Cu^{2+}, Cd^{2+}, Ni^{2+}, Mn^{2+}, and Zn^{2+}) were analyzed with an atomic absorption spectrometer, PerkinElmer AA 800, using APHA standardized methods. Calibration curves with a correlation index $R \geq 99\%$ were run before analyzing each sample. For the analysis of anions such as CrO_4^{2-} (Cr^{6+}), an ion chromatograph Dionex ICS 1100, equipped with a guard column AG14 and an analytical column AS14, both of 4 mm, and a sample loop of 50 μL, was used. A solution of 35 mM sodium hydroxide was used as the eluent solution.

3. Results and Discussion

3.1. Characterization of Multicomponent Nanoparticles. A TEM image showed a spherical morphological structure (Figure 1(a)). The nanoparticle size distribution was obtained with a dynamic light scattering (DLS). The Gaussian distribution with an average size of polydispersed nanoparticles lies in a range of 9.5 ± 1.5 nm in diameter (Figure 1(c)). The size of the nanoparticles was similar to that obtained with TEM. Roughness of nanoparticles was estimated using MATLAB software developed by Arroyo et al. [19]. This software calculated roughness as a fractal dimension (Figures 1(b) and 1(d)), and the value was given as 1.8 (Ds = 1.8). Gagnepain and Roques-Carmes exploited this technique to characterize the uniformity of surfaces for profiles in two dimensions, with Ds falling within a range between 1 and 2, in which 1 corresponds to a smooth surface and 2 to a highly rough surface [20]. Recently, in the fabrication of Fe/FeS nanoparticles was evidenced an enhancement in roughness of the particles' surfaces [7, 8]. Evidently, a high roughness favors the reactivity of the nanoparticle due to the increase of its surface area, thus promoting the formation of more reactive sites [7, 21]. Figure 2(a) shows the UV-Vis spectrum of the mortiño berry extract. Two broad peaks between 240 and 340 nm and 480 and 530 nm were observed, which are related to the presence of gallic acid, vanillic acid, hydroxybenzoic acid,

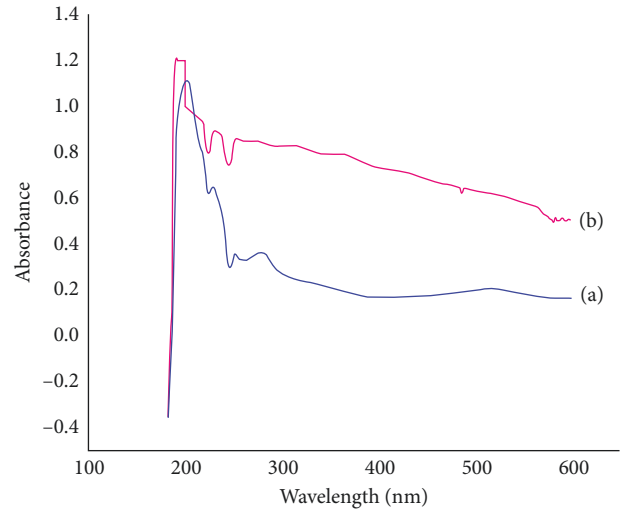

Figure 2: UV-Vis spectra of (a) the mortiño berry extract and (b) as-prepared multicomponent nanoparticles.

caffeic/ferulic acid, chlorogenic acid, coumaric acid, myricetin, quercetin, delphinidin, and cyanidin [15, 16, 22].

The as-synthesized multicomponent nanoparticles (Figure 2(b)) showed a broad contribution in the visible light, in addition to the strong band at ~200 nm and the small one at ~240 nm. As reported by Sherman and Waite [23], species based on iron oxides and hydroxides have four predominant regions of absorption: ligand to metal charge transfer (250–400 nm) along with contribution of Fe^{3+} ligand field transition (290–310 nm), pair excitation process (400–600 nm) of magnetically coupled Fe^{3+} ions, and two strong absorption bands near 640 and 900 nm of ligand field transitions of Fe^{3+} cation in the octahedral environment. The peak found at 290 nm is related to the formation of iron oxide nanoparticles [24] mediated by complex polyphenols contained in the mortiño extract. Recently, these polyphenols induced the reduction of silver ions to metallic silver during the synthesis of the silver-graphene nanocomposite [22]. A peak at 270 nm corresponding to the oxidized polyphenols can also be shown. This peak emerges on the as-synthesized nanoparticle spectrum due to the limitations of the antioxidant activity of the fruit extract. Additionally, peaks from 210 to 260 nm are seen in the two analyzed samples, and it is suggested that they resemble the presence of polyphenols. Markova et al. [25] biosynthesized nanoparticles with green tea leaves and compared with nanoparticles synthesized with sodium borohydride. Nanoparticles prepared with green tea leaves showed peaks at 210, 220, and 270 n, whereas in the inorganic samples (nanoparticles with sodium borohydride), these peaks do not show up. Moreover, XRD analyses revealed that the as-synthesized nanoparticles contain iron oxides in the core and a small amount of iron sulfide on the surface as shown in Figure 3. Peaks at 35.54° and 75.3° matched to iron oxides and the peak at 34.03° corresponded to iron sulfide. Benitez in 2010 found iron oxides linked to peaks at 31° and 45.5° [26]. Nevertheless, the displacement of the positions of peaks observed in the study is due to the synthesis protocol. Lastly, FTIR measurements were carried out to understand the

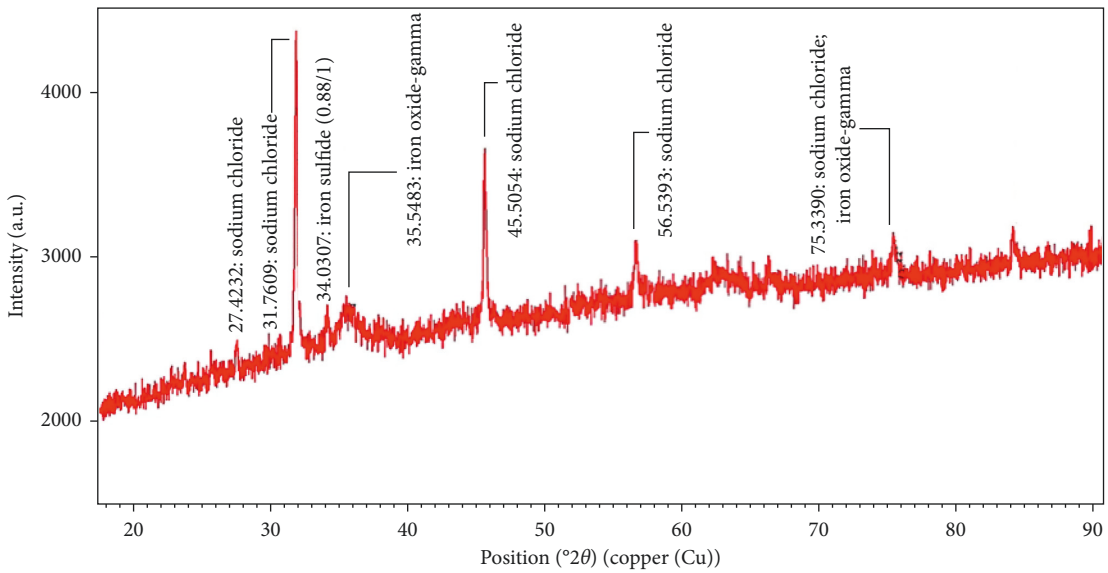

Figure 3: XRD spectrum of multicomponent nanoparticles.

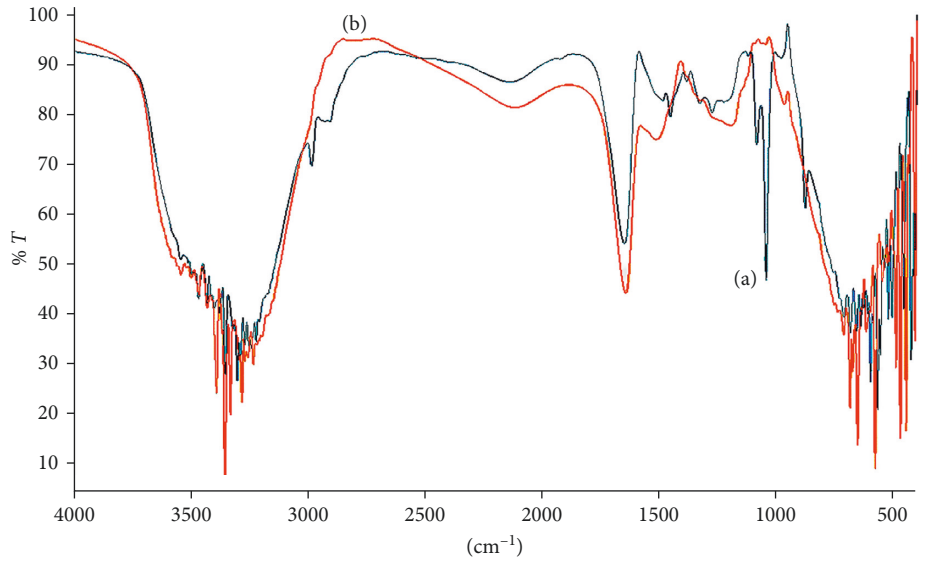

Figure 4: FTIR spectra of (a) the mortiño berry extract and (b) as-prepared multicomponent nanoparticles.

participation of the MBE molecules in the formation of nanoparticles. As seen in Figure 4(a), peaks in the range of 3650–3200 cm^{-1} are related to the vibrations of the –OH groups of the phenolic moiety of MBE, and positions from 1620 to 1690 cm^{-1} are attributed to the aldehydes (C=O) of an ester sugar. These peaks in conjunction with the 1089 cm^{-1} peak (CO stretching) represent the amount of carbon that belongs to the extract. Conversely, the peaks observed at positions 577 and 489–826 cm^{-1} are characteristic of the vibrations produced by iron oxides (FeO) and sulphides (S–S), respectively (Figure 4(b)). Herlekar and Palanisamy et al. studied the formation of peaks for Fe–O (636.16–550 cm^{-1}) using the FTIR technique [27, 28]. The peak appearing in the spectrum of multicomponent nanoparticles (577 cm^{-1}) is in between the given peaks, while peaks at 489 and 826 cm^{-1} are attributed to the vibrations of sulphides. A previous study locates FTIR peaks at 480 cm^{-1} and 600 cm^{-1} for the sulfide group [29]. Therefore, it can be suggested that multicomponent nanoparticles were actually formed.

3.2. Kinetic Study. Figure 5 shows results of kinetic tests for the removal of heavy metals from artificially contaminated water using multicomponent nanoparticles (FexO/FeS). It is observed that most of metals achieved maximum removal after 5 min (99.8% Cu, 99.5% Zn, 99.6% Ni, 71.4% Mn, 99.6% Cd, and 99% Cr), showing a sharp slope and then reaching the steady state at around 60 min.

Also, it is seen that there is no difference in the removal rate for each metal. It is remarkable to mention that kinetic

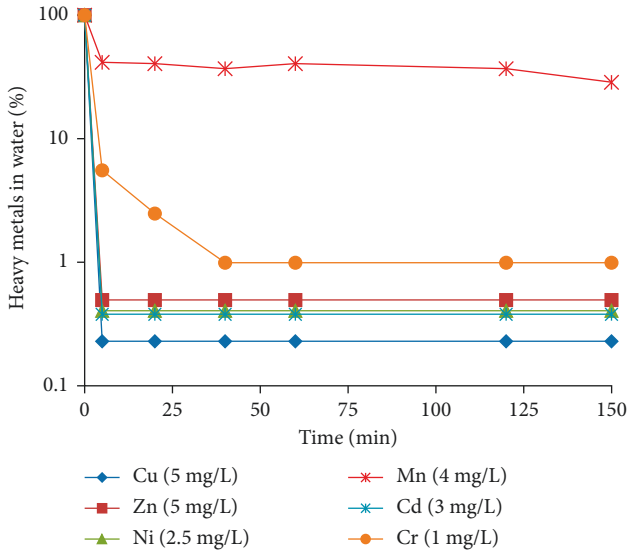

Figure 5: Kinetic profiles of heavy metals in artificially contaminated water treated with multicomponent nanoparticles.

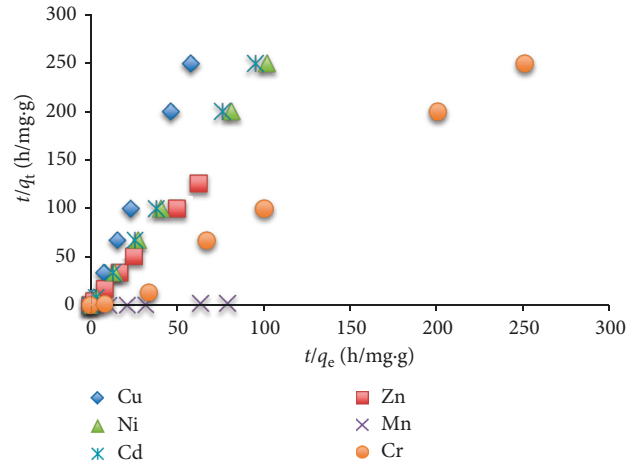

Figure 6: Pseudo-second order kinetics for the uptake of heavy metals from water.

data for the adsorption of heavy metals fit very well a pseudo-second-order model (2) as seen in Figure 6:

$$\frac{t}{q_t} = \frac{1}{k_2 q_e^2} + \frac{1}{q_e} t, \quad (2)$$

where k_2 (g/mg·h) is the pseudo-second-order rate constant, q_e is the amount of metal adsorbed (mg/g) at equilibrium, and q_t is the amount of the adsorption (mg/g) at any time t (h) [30]. All fitting curves showed good linearity with a correlation factor equal to unity ($R^2 = 1$). As observed in Figure 5, there was not any change in the concentration of heavy metals in the time period between 5 and 60 min. This implies that chemisorption is the principal mechanism for the uptake of heavy metals [31–33]. However, the electronegativity and the hydrated ionic size of the metallic elements play the role in the selectivity of the adsorption [34]. For example, in our study, the hydrated radius of Mn^{2+} is larger than that of Cu^{2+} ($Mn^{2+} r_H = 0.438$ nm and $Cu^{2+} r_H = 0.419$ nm) [35] difficulting coulumbic interactions of Mn with the reactive sites of nanoparticles. Also, Mn is the element with the least electronegativity in the series of the studied metals (Mn = 1.55) [36]. Therefore, its tendency to attract electrons is less, which in turn decreases the interactions with the nanoparticles. Also, precipitate formation of metallic sulfides speeds up the removal of heavy metals from water [37–40]. In previous studies of our group, it is reported that multicomponent nanoparticles of zerovalent iron and iron sulfide (Fe/FeS) rapidly removed heavy metals from an artificially prepared mine tailing due to processes of physisorption and chemisorption [8].

3.3. Simultaneous Immobilization of Heavy Metals in Fixed-Bed Columns. A simultaneous immobilization of heavy metals was performed in a fixed-bed column packed with 2.0 g of soil (properties in Table S1) and treated with MCNPs. In Figure 7 is shown that immobilization of heavy metals is

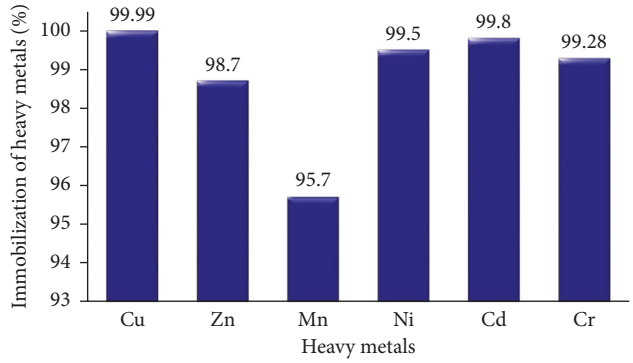

Figure 7: Heavy metal immobilization in 2 g of soil at pH 6.58 using 5 mL of MCNPs

higher than 95%. However, the distribution of heavy metals in the soil fractions changed after treatment. Nickel, copper, cadmium, chromium, zinc, and manganese (Figures 8(a)–8(f)) decreased in concentration in the exchangeable phase (22.1%, 9%, 7.9%, 2.6%, 1.82%, and 0.6%, resp.), while Ni^{2+}, Cu^{2+}, and Cd^{2+} showed an increase in concentration in the oxidable fraction (9.1% 3.3.7%, and 2.6%, resp.) (Figures 8(a)–8(c)).

On the contrary, concentrations of Ni^{2+} and Cd^{2+} (Figures 8(a) and 8(c)) were higher than those of Cu^{2+} and Cr^{6+} (Figures 8(b) and 8(d)) in the reducible phase after treatment of soils. The drop in the exchangeable fraction could be related to a rapid capture of the toxic cations from soil by MCNPs, forming metallic sulfide precipitates and therefore increasing the oxidable phase. In harmony with Figure 3, multicomponent nanoparticles contain FeS and iron oxides. Once FeS thin film contacted with free heavy metals in the pore water of soil samples, S^{2-} promptly reacted with the toxic metals, forming chemically stable sulfides [41–43] because their solubility products favored the reaction ($K_{sp,Cu} = \sim 10^{-47}$; $K_{sp,Cd} = \sim 10^{-29}$; and $K_{sp,Ni} = \sim 10^{-12}$) [44]. Additionally, concentration of ions with E^0 values close to Fe^{2+} ($E^0 = -0.44$ V) may be lowered much less to reducible forms ($Ni^{2+} = -0.25$ V, $Cd^{2+} = -0.4$ V)

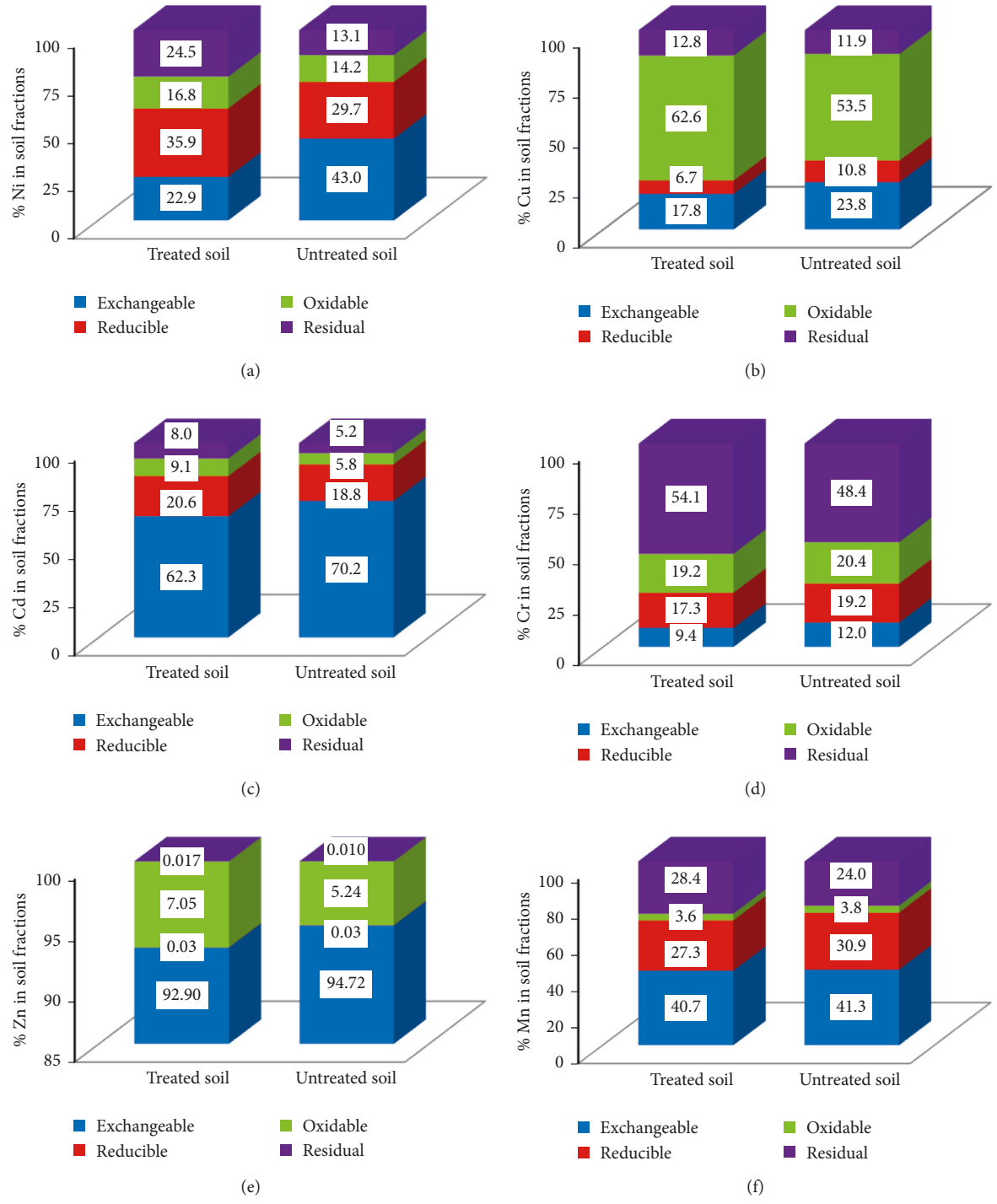

FIGURE 8: Distribution of heavy metals in soils after treatment (T) using 2 g of soil and 5 mL of MCNPs at pH 6.58 and without treatment (UT): (a) Ni, (b) Cu, (c) Cd, (d) Cr, (e) Zn, and (f) Mn.

compared to that of ions with higher reduction potential ($Cu^{2+} = +0.337$ V and $Cr^{6+} = +1.33$ V) [45]. As result, Ni^{2+} and Cd^{2+} are increased in the reducible fraction, whereas Cu^{2+} and Cr^{6+} (CrO_4^{2-}) decreased. As indicated before, MCNPs also contain iron oxides in the core. These metallic oxides in the pore water could easily release Fe^{2+} or form hydrated iron oxides [46]. Also, Fe^{2+} ions from the ionization of FeS were in the pore water. Hence, both sources of Fe^{2+} could trigger reduction of toxic metallic ions.

3.4. Leaching of Heavy Metals from Treated Soils. Leaching test results of soils treated with nanoparticles and without treatment under different extractive solutions are observed

Table 1: Percentage of heavy metals leaching from soil samples.

Metal	Rainwater		Drinking water		Deionized water		Acidified water	
	T	UT	T	UT	T	UT	T	UT
Cu	0	3.0	0.1	1.3	0.2	4.2	16.0	47.1
Zn	0.6	17.0	0.9	17.2	1.4	19.6	46.5	89.6
Ni	5.2	8.9	1.5	5.0	1.4	3.6	53.8	88.4
Mn	1.7	3.7	4.6	5.3	1.8	4.7	64.5	70.9
Cd	0.0	0.6	0.0	0.1	0.0	0.3	2.0	5.7
Cr	15.8	16.3	13.3	23.7	17.1	21.7	19.4	46.4

T: treated soil with MCNPs; UT: untreated soil with MCNPs.

in Table 1. In general, concentration of heavy metals in the aqueous phase (free metals) is lower for soils treated with MCNPs. However, when acidic water (pH ~ 2) was used as the extracting fluid, the release of heavy metals from soils increased. Zn^{2+}, Cr^{6+}, and Mn^{2+} were the most soluble metals in the extractant medium. Acidic liquids reacting with soils are more aggressive initiating accelerated leaching of heavy metals [47, 48]. At pH < 5, the mobility of metals is improved as a result of the higher concentration of competing protons [49, 50].

4. Conclusion

Kinetic tests revealed a high reactivity of the multicomponent nanoparticles for the removal of heavy metals from artificially contaminated water. This removal is regarded to both physisorption and chemisorption processes. The initial uptake is a physical phenomenon, and it requires only five minutes to remove more than 90% of all heavy metals existing in the aqueous phase. The completion of the reaction takes around 60 min without any leaching of metallic elements due to a chemisorption uptake. On the other hand, the effluent of the column packed with contaminated soils treated with MCNPs showed minimal concentration of heavy metals after five days. All heavy metals were well immobilized within the soil matrix. Nevertheless, the distribution in the soil fractions varies after treatment. In general, the amount of heavy metals in the exchangeable phase decreased, while copper, cadmium, and nickel increased in the oxidable fraction. In contrast, concentrations of nickel and cadmium were higher than those of copper and chromium in the reducible phase. As reported, immobilization of the toxic metals in soil was a successful procedure; metals do not leach even when flowing rainwater, drinking water, and deionized water through the soil. Yet, leaching of heavy metals is moderate when acidic water is used as an extracting solution.

Conflicts of Interest

The authors declare that they have no conflicts of interest.

Acknowledgments

The authors thank Dr. Alexis Debut for the TEM images, Dr. Carlos Arroyo for allowing us to use his software for estimating the fractal dimension of roughness, and Mr. Gustavo Martínez for preparing the graphical material. Thanks also to the Universidad de las Fuerzas Armadas for providing funds through a research project.

Supplementary Materials

Table S1: the chemical and physical properties of soil without treatment. (*Supplementary Materials*)

References

[1] R. G. Chaudhuri and S. Paria, "Core/shell nanoparticles: classes, properties, synthesis mechanisms, characterization, and applications," *Chemical Reviews*, vol. 112, no. 4, pp. 2373–2433, 2011.

[2] B. Issa, I. M. Obaidat, B. A. Albiss, and Y. Haik, "Magnetic nanoparticles: surface effects and properties related to biomedicine applications," *International Journal of Molecular Sciences*, vol. 14, no. 11, pp. 21266–21305, 2013.

[3] J. Tian, J. Xu, F. Zhu, T. Lu, C. Su, and G. Ouyang, "Application of nanomaterials in sample preparation," *Journal of Chromatography A*, vol. 1300, pp. 2–16, 2013.

[4] J. E. Hutchison, "Greener nanoscience: a proactive approach to advancing applications and reducing implications of nanotechnology," *ACS Nano*, vol. 2, no. 3, pp. 395–402, 2008.

[5] B. Zhou, S. Parasher, and M. Rueter, "Multicomponent nanoparticles formed using a dispersing agent," US Patent no. 7,632,775, December 2009.

[6] H. Zeng and S. Sun, "Syntheses, properties, and potential applications of multicomponent magnetic nanoparticles," *Advanced Functional Materials*, vol. 18, no. 3, pp. 391–400, 2008.

[7] E. J. Kim, J. H. Kim, A. M. Azad, and Y. S. Chang, "Facile synthesis and characterization of Fe/FeS nanoparticles for environmental applications," *ACS Applied Materials & Interfaces*, vol. 3, no. 5, pp. 1457–1462, 2011.

[8] L. H. Cumbal, A. Debut, D. Delgado, C. Bastidas, and C. Stael, "Synthesis of multicomponent nanoparticles for immobilization of heavy metals in aqueous phase," *Nano World Journal*, vol. 1, no. 4, pp. 103–109, 2015.

[9] D. N. Tran, S. Kabiri, and D. Losic, "A green approach for the reduction of graphene oxide nanosheets using non-aromatic amino acids," *Carbon*, vol. 76, pp. 193–202, 2014.

[10] S. F. Adil, M. E. Assal, M. Khan, A. Al-Warthan, M. R. H. Siddiqui, and L. M. Liz-Marzán, "Biogenic synthesis of metallic nanoparticles and prospects toward green chemistry," *Dalton Transactions*, vol. 44, no. 21, pp. 9709–9717, 2015.

[11] S. Iravani, "Green synthesis of metal nanoparticles using plants," *Green Chemistry*, vol. 13, no. 10, pp. 2638–2650, 2011.

[12] M. J. Firdhouse and P. Lalitha, "Phyto-reduction of graphene oxide using the aqueous extract of *Eichhornia crassipes* (Mart.) Solms," *International Nano Letters*, vol. 4, no. 4, pp. 103–108, 2014.

[13] T. Kuila, S. Bose, P. Khanra, A. K. Mishra, N. H. Kim, and J. H. Lee, "A green approach for the reduction of graphene oxide by wild carrot root," *Carbon*, vol. 50, no. 3, pp. 914–921, 2012.

[14] A. H. Al-Marri, M. Khan, M. Khan et al., "*Pulicaria glutinosa* extract: a toolbox to synthesize highly reduced graphene oxide-silver nanocomposites," *International Journal of Molecular Sciences*, vol. 16, no. 1, pp. 1131–1142, 2015.

[15] C. Vasco, K. Riihinen, J. Ruales, and A. Kamal-Eldin, "Chemical composition and phenolic compound profile of

mortiño (*Vaccinium floribundum* Kunth)," *Journal of Agricultural and Food Chemistry*, vol. 57, no. 18, pp. 8274–8281, 2009.

[16] G. A. Garzón, C. E. Narváez, K. M. Riedl, and S. J. Schwartz, "Chemical composition, anthocyanins, non-anthocyanin phenolics and antioxidant activity of wild bilberry (*Vaccinium meridionale* Swartz) from Colombia," *Food Chemistry*, vol. 122, no. 4, pp. 980–986, 2010.

[17] O. Heiri, A. F. Lotter, and G. Lemcke, "Loss on ignition as a method for estimating organic and carbonate content in sediments: reproducibility and comparability of results," *Journal of Paleolimnology*, vol. 25, no. 1, pp. 101–110, 2001.

[18] A. M. Ure, P. Quevauviller, H. Muntau, and B. Griepink, "Speciation of heavy metals in soils and sediments. An account of the improvement and harmonization of extraction techniques undertaken under the auspices of the BCR of the Commission of the European Communities," *International Journal of Environmental Analytical Chemistry*, vol. 51, no. 1-4, pp. 135–151, 1993.

[19] C. R. Arroyo, A. Vaca, A. Debut, and L. Cumbal, "Reliable tools for quantifying the morphological properties at the nanoscale," *Biology and Medicine*, vol. 8, no. 3, pp. 1–7, 2016.

[20] J. J. Gagnepain and C. Roques-Carmes, "Fractal approach to two-dimensional and three-dimensional surface roughness," *Wear*, vol. 109, no. 1–4, pp. 119–126, 1986.

[21] E. Malkoc and Y. Nuhoglu, "Removal of Ni(II) ions from aqueous solutions using waste of tea factory: adsorption on a fixed-bed column'," *Journal of Hazardous Materials*, vol. 135, no. 1–3, pp. 328–336, 2006.

[22] K. S. Vizuete, B. Kumar, A. V. Vaca, A. Debut, and L. Cumbal, "Mortiño (*Vaccinium floribundum* Kunth) berry assisted green synthesis and photocatalytic performance of silver–graphene nanocomposite," *Journal of Photochemistry and Photobiology A: Chemistry*, vol. 329, pp. 273–279, 2016.

[23] D. M. Sherman and T. D. Waite, "Electronic spectra of Fe^{3+} oxides and oxide hydroxides in the near IR to near UV," *American Mineralogist*, vol. 70, pp. 1262–1269, 1985.

[24] H. Muthukumar and M. Matheswaran, "*Amaranthus spinosus* leaf extract mediated FeO nanoparticles: physicochemical traits, photocatalytic and antioxidant activity," *ACS Sustainable Chemistry & Engineering*, vol. 3, no. 12, pp. 3149–3156, 2015.

[25] Z. Markova, P. Novak, J. Kaslik et al., "Iron(II, III)–polyphenol complex nanoparticles derived from green tea with remarkable ecotoxicological impact," *ACS Sustainable Chemistry & Engineering*, vol. 2, no. 7, pp. 1674–1680, 2014.

[26] M. J. Benitez, D. Mishra, P. Szary et al., "Structural and magnetic characterization of self-assembled iron oxide nanoparticle arrays," *Journal of Physics: Condensed Matter*, vol. 23, no. 12, p. 126003, 2011.

[27] M. B. Herlekar, "Biological synthesis of iron oxide nanoparticles using agro-wastes and feasibility for municipal wastewater treatment," in *Proceedings of the 47th Indian Water Works Association (IWWA) Convention*, Kolkata, West Bengal, India, January-February 2015.

[28] K. L. Palanisamy, V. Devabharathi, and N. M. Sundaram, "The utility of magnetic iron oxide nanoparticles stabilized by carrier oils in removal of heavy metals from waste water," *International Journal of Research in Applied, Natural and Social Sciences*, vol. 1, no. 4, pp. 15–22, 2013.

[29] F. L. Pua, C. H. Chia, S. Zakari et al., "Preparation of transition metal sulfide nanoparticles via hydrothermal route," *Sains Malaysiana*, vol. 39, no. 2, pp. 243–248, 2010.

[30] J. Gong, T. Liu, X. Wang, X. Hu, and L. Zhang, "Efficient removal of heavy metal ions from aqueous systems with the assembly of anisotropic layered double hydroxide nanocrystals@carbon nanosphere," *Environmental Science & Technology*, vol. 45, no. 14, pp. 6181–6187, 2011.

[31] S. D. Comber, M. J. Gardner, A. M. Gunn, and C. Whalley, "Kinetics of trace metal sorption to estuarine suspended particulate matter," *Chemosphere*, vol. 33, no. 6, pp. 1027–1040, 1996.

[32] Y. S. Ho and G. McKay, "The kinetics of sorption of divalent metal ions onto sphagnum moss peat," *Water Research*, vol. 34, no. 3, pp. 735–742, 2000.

[33] Y. S. Ho, J. C. Ng, and G. McKay, "Removal of lead(II) from effluents by sorption on peat using second-order kinetics," *Separation Science and Technology*, vol. 36, no. 2, pp. 241–261, 2001.

[34] E. Sočo and J. Kalembkiewicz, "Removal of copper(II) and zinc(II) ions from aqueous solution by chemical treatment of coal fly ash," *Croatica Chemica Acta*, vol. 88, no. 3, pp. 267–279, 2015.

[35] E. R. Nightingale, "Phenomenological theory of ion solvation. Effective radii of hydrated ions," *Journal of Physical Chemistry*, vol. 63, no. 9, pp. 1381–1387, 1959.

[36] A. L. Allred, "Electronegativity values from thermochemical data," *Journal of Inorganic and Nuclear Chemistry*, vol. 17, no. 3-4, pp. 215–221, 1961.

[37] D. T. Rickard, "Kinetics and mechanism of pyrite formation at low temperatures," *American Journal of Science*, vol. 275, no. 6, pp. 636–652, 1975.

[38] G. W. Luther, "Pyrite synthesis via polysulfide compounds," *Geochimica et Cosmochimica Acta*, vol. 55, no. 10, pp. 2839–2849, 1991.

[39] D. Rickard and G. W. Luther, "Kinetics of pyrite formation by the H_2S oxidation of iron(II) monosulfide in aqueous solutions between 25 and 125°C: the mechanism," *Geochimica et Cosmochimica Acta*, vol. 61, no. 1, pp. 135–147, 1997.

[40] D. Rickard, "Kinetics of pyrite formation by the H_2S oxidation of iron(II) monosulfide in aqueous solutions between 25 and 125°C: the rate equation," *Geochimica et Cosmochimica Acta*, vol. 61, no. 1, pp. 115–134, 1997.

[41] J. G. Dean, F. L. Bosqui, and K. H. Lanouette, "Removing heavy metals from waste water," *Environmental Science & Technology*, vol. 6, no. 6, pp. 518–522, 1972.

[42] R. G. Lidzey, J. H. P. Watson, and D. C. Ellwood, "The removal of the pertechnetate ion and actinides from radioactive waste streams at Hanford, Washington, USA and Sellafield, Cumbria, UK: the role of iron-sulfide-containing adsorbent materials," *Nuclear Engineering and Design*, vol. 226, no. 3, pp. 375–385, 2003.

[43] R. D. Ludwig, R. G. McGregor, D. W. Blowes, S. G. Benner, and K. Mountjoy, "A permeable reactive barrier for treatment of heavy metals," *Ground Water*, vol. 40, no. 1, pp. 59–66, 2002.

[44] R. Chang and K. A. Goldsby, *General Chemistry: The Essential Concepts*, McGraw-Hill, New York, NY, USA, 7th edition, 2014.

[45] J. E. Macdonald and J. G. C. Veinot, "Removal of residual metal catalysts with iron/iron oxide nanoparticles from coordinating environments," *Langmuir*, vol. 24, no. 14, pp. 7169–7177, 2008.

[46] A. K. Gupta and M. Gupta, "Synthesis and surface engineering of iron oxide nanoparticles for biomedical applications," *Biomaterials*, vol. 26, no. 18, pp. 3995–4021, 2005.

[47] J. J. Dijkstra, J. C. L. Meeussen, and R. N. J. Comans, "Leaching of heavy metals from contaminated soils: an experimental and modeling study," *Environmental Science & Technology*, vol. 38, no. 16, pp. 4390–4395, 2004.

[48] S. A. Zheng, X. Zheng, and C. Chen, "Leaching behavior of heavy metals and transformation of their speciation in polluted soil receiving simulated acid rain," *PLoS One*, vol. 7, no. 11, Article ID e49664, 2012.

[49] E. O. E. Agbenyeku, E. Muzenda, and M. L. Msibi, "Chemical alterations in three clayey soils from percolation and interaction with acid mine drainage (AMD)," *South African Journal of Chemical Engineering*, vol. 21, pp. 28–36, 2016.

[50] P. H. T. Beckett, "The use of extractants in studies on trace metals in soils, sewage sludges, and sludge-treated soils," in *Advances in Soil Science*, pp. 143–176, Springer, New York, NY, USA, 1989.